

Initial Growth and Texture Formation during Reactive Magnetron Sputtering of TiN on Si (111)

T.Q. Li*, S. Noda, Y. Tsuji, T. Ohsawa, and H. Komiyama

Department of Chemical System Engineering, University of Tokyo,

7-3-1 Hongo, Bunkyo-ku, Tokyo 113-8656, JAPAN

Phone: +81-3-5841-7318, Fax: +81-3-5841-7230, E-mail: litg@chemsys.t.u-tokyo.ac.jp

Abstract

Titanium nitride (TiN) films were grown on (111) silicon substrates by using reactive magnetron sputtering of a titanium metallic target under a N₂/Ar atmosphere, and analyzed in detail by using transmission electron microscopy (TEM) and X-ray diffraction (XRD). Two power sources for the sputtering, d.c. and r.f., were compared. At the initial growth stage, a continuous film containing randomly oriented nuclei was observed when the film thickness was about 3 nm. The nuclei grew and formed a polycrystalline layer when the film thickness was about 6 nm. As the film grew further, its orientation changed depending on the deposition conditions. For d.c. sputtering, the existence of (111) or (200)-preferred orientations depended on the N₂ partial pressure, and the intensity of the preferred orientation increased with increasing film thickness. For r.f. sputtering, however, when the film thickness was about 20 nm, the film showed (200) orientation independent of the N₂ partial pressure, and further growth caused the film to orient to the (111) orientation when the N₂ partial pressure was low (< 0.015Pa). The results indicate that TiN preferred orientation is controlled by a competition between kinetic and thermodynamic effects.

I. INTRODUCTION

TiN are widely used as diffusion barriers for Al-based interconnects in multilevel interconnections incorporated in submicron ultra large-scale integrated (ULSI) device. As the dimensions of integrated circuits continue to decrease with increasing packing density, the thickness of metal interconnect layers and diffusion barriers continue to decrease. To reduce the electrical resistivity of the barrier/metal structure, the thickness of diffusion barriers is expected to be reduced to less than 10 nm [1]. To control the structure and properties of such thin barrier layers, the initial growth mechanism must be understood.

It is known that the preferred orientation of thin films is important in their applications. For example, electromigration lifetime of Al metal lines can be enhanced by strong (111) orientation of Al [2-6]. A strongly (111) textured TiN underlayer induces a similarly strong (111) texture in the Al upper-layer [5,7,8]. However, TiN films with thickness of tens of nanometers are often reported to have (200) preferred orientations, the (111) orientation appears only when the films have a thickness above hundreds of nanometers [9-11]. Pelleg et al. [10] suggested that the TiN preferred orientation is controlled by the competition between the surface free energy and the strain energy. By assuming that the strain energy in the film increases linearly with thickness, they postulated that when the film thickness is sufficiently small, the film orientation is that for a film with minimum surface energy, which has been observed to be (100) for TiN films [10]. As the film grows past a critical thickness, the strain energy exceeds the surface energy. Because the elastic moduli, E , of TiN are anisotropic with $E_{100} > E_{111}$, the preferred orientation of TiN films will evolve toward an (111) orientation. This suggests that it is difficult to fabricate TiN (111)-oriented films at small thickness.

On the other hand, Patsalas et al. [12] reported that when the internal stress was increased from 0.3 GPa to 2 GPa by increasing the substrate bias voltage, the preferred TiN orientation changed from (111) to (200). This result conflicts with the analysis by Pelleg et al. and implies

that the strain energy might not be the main cause for the (111) preferred orientation. To clarify the mechanism that causes the formation of the (111) and (200) film orientations, we investigated the initial growth stage and texture evolution of TiN film by using transmission electron microscopy (TEM) and X-ray diffraction (XRD), and compared the results derived from the d.c. and r.f. power sources for the sputtering. Based on our results, we developed a model from the viewpoint of the competition between the thermodynamic equilibrium and kinetics to explain the formation of TiN preferred orientation.

II. EXPERIMENTAL

The TiN thin films were reactive sputter-deposited using a titanium target in a N₂/Ar atmosphere in a combined d.c. and r.f. magnetron sputtering system. The sputter chamber was equipped with a load-lock system and pumped with a cryo pump, and had a base pressure of 5×10⁻⁶ Pa. The target was a 2-inch-diameter, 99.99% pure Ti disc. The substrates were (111) Si wafers. Before being loaded into the loading chamber, the wafers were treated chemically in a mixture of concentrated sulphuric acid and H₂O₂, and then cleaned in a 1% HF solution to remove the contaminants and the native SiO₂ layer on the surface. The sputtering gases, N₂ and Ar, were controlled with independent mass-flow controllers, and mixed before they were introduced into the chamber. Before deposition the target was pre-sputtered in the Ar gas for 5 min. During the deposition, the total pressure in the sputtering chamber was 0.93 Pa, the substrate to target distance was 50mm, and the discharge power to the Ti target was either 69 W d.c. or 100 W r.f. The samples for TEM observation were deposited a 10 nm SiO₂ layer just after the deposition of TiN, to avoid oxidation of TiN layer and to immobilize it against the irradiation of the electron beam during TEM observation.

The microstructure of the films was investigated with XRD (Rigaku RINT2400) using CuK α radiation, and with plan-view and cross-sectional TEM (Jeol, JEM2010F). The

plan-view specimen was prepared first by cut the SiO₂/TiN/Si sheet into a 3 mm disc, and then grinding and polishing from the Si side down to about 100 μm thick. The cross-sectional specimen was prepared by gluing two 7 x 7 mm square specimens face-to-face, and then cutting perpendicular to the film-substrate interface into slices about 1 mm thick. After grinding and polishing, the thickness was thinned down to about 100 μm.

Before ion milling, both types of specimen were dimpled by a precision grinding machine. Ion milling was done at 4 kV, at a milling angle of 6 °. For the plan-view specimen, the milling process was carried out from the Si side, while for the cross-sectional specimen, it was milled from both sides to the thickness that can be used for TEM observation.

The film thickness was measured with a stylus profilometer (KLA-Tencor P-10). The film composition was determined with in-situ Auger Electron Spectroscopy (AES) and Rutherford Backscattering Spectrometry (RBS).

III. RESULTS AND DISCUSSION

Ultimate films: Effect of N₂ partial pressure and sputter power sources

We determined the deposition conditions to obtain stoichiometric TiN films with good crystallinity by varying N₂ partial pressures of the sputtering gases for both d.c. and r.f. sputtering. The results (Fig. 1) show that the deposition rate decreased with increasing N₂ partial pressure. This decrease is due to the difference in the sputtering yield between N₂ and Ar ions and to the decrease in sputtering yield caused by the nitridation of Ti to TiN on the Ti target surface.

The XRD patterns of TiN films deposited under various N₂ partial pressures are shown in Figure 2. Figures 2a and 2b show the results of 50-nm-thick films deposited by d.c. sputtering and 100-nm-thick films deposited by r.f. sputtering, respectively. In both figures, XRD patterns show the same trend that, for an increase in N₂ partial pressure from 0.015 Pa to 0.47

Pa, the preferred orientations of the films changed from TiN (111) to TiN (200), whereas AES or RBS measurements indicated that the Ti/N ratio remained stoichiometric. This same trend was also reported by H. H. Yang et al. [13] and Li-Jian Meng et al. [14] Based on our results, the deposition conditions used to investigate the initial growth mechanism of TiN were determined by setting the N₂ partial pressure to 0.047 Pa for d.c. sputtering and to 0.015 Pa for r.f. sputtering, at which we obtained the (111) oriented ultimate films represented in Fig. 2. The deposition conditions are shown in detail in Table 1.

Film thickness less than 10 nm (initial growth stage): Formation of randomly oriented polycrystalline layer

We investigated the initial growth stage of TiN films by using TEM. Figure 3 shows the cross-section and plan-view of TEM images of TiN deposited for 10 s by using d.c. sputtering (Condition I). From the different contrast between the TiN layer and the upper SiO₂ layer, Figure 3a shows a continuous TiN layer, inside which small crystal grains about 2-3 nm in diameter were found. The matrix surrounding the crystal grains is supposed to be amorphous phase with the mazy contrast, as shown in Fig. 3a and Fig. 3b. From these results, we suppose that nucleation occurred in the continuous amorphous layer in its initial stage, differently from the traditional island growth mode, determined by using resonant nuclear reaction before [15].

Figure 4a shows an image of the 30-s deposition TiN film (Condition I). The grains grew to about 6 nm in diameter, and then came in contact with each other, thus forming a continuous polycrystalline layer. Lattice imaging shows that the lattice parameters for this film were identical to those for TiN (lattice parameters shown in Fig. 4a). To determine if each grain had a preferred orientation, nano-beam diffraction patterns were obtained for 20 randomly sampled grains. No preferred orientations were found in these patterns. The cross-sectional lattice images shown in Fig. 4a also indicate that the grains were randomly

oriented.

The growth of films deposited by using r.f. sputtering was similar to films deposited by using d.c. sputtering. First, TiN thin films at the initial stage consisted of small crystal grains embedded in a continuous TiN layer. Then, the grains grew and came in contact with each other, thus forming randomly oriented polycrystalline layer.

Film thickness up to 50 nm: Evolution of (200) or (111) preferred orientation

Figure 4b shows that as the deposition time increased to 120 s under Condition I, the film became columnar. The grains on the bottom of the film were still randomly oriented, whereas those on the top of the film were dominantly oriented in the (111) direction.

The effect of film thickness greater than 17 nm on orientation was investigated by using XRD. Figure 5a shows the XRD for films deposited by using d.c. sputtering. The films showed weak, (111) preferred orientation at a thickness of either 17 or 23 nm, with a weaker (200) peak. This much weak (200) peak indicates the initial, randomly oriented grains. This result coincides with the TEM image shown in Fig. 4b. The intensity of the (111) peak increased as the film thickness increased to 50 nm.

In contrast, Fig. 5b shows that the films deposited by using r.f. sputtering showed (200) preferred orientation at a film thickness of 19 nm. Then the intensity of the (111) peak increased rapidly with increasing film thickness, whereas that of the (200) peak remained relatively constant. When the film thickness reached 110 nm, Fig. 5b indicates that the preferred orientation of the film changed from (200) to (111).

The effect of film thickness on film orientation is summarized in Table 2. Based on these results, we developed a model from both the viewpoints of kinetics and thermodynamics to qualitatively explain the evolution of the film orientation.

IV. MODEL OF EVOLUTION OF ORIENTATION IN TiN FILMS

Figure 6 shows a schematic of TiN film growth. At the beginning of deposition, the deposition species includes mostly titanium and nitrogen atoms and ions, [16-17] which reach the surface of the crystalline silicon substrate and form an amorphous layer. Although details of the formation mechanism of the amorphous phase remain unclear, this phase probably forms because, for nano-scale film thickness, the amorphous phase is more stable than the crystal phase. When the film thickness exceeds a critical value, nucleation occurs inside the amorphous layer.

Generally, nuclei are classified into two types, wetting-mode and non-wetting-mode nuclei, according to their wettability on substrate. The wetting-mode nuclei have a small contact angle (near 0°) and a large contact area with the substrate (shown in Fig. 6b). Due to their larger upside area, wetting-mode nuclei have an orientation that affects the surface energy of the film. On the other hand, non-wetting-mode nuclei have a large contact angle (near 180°) and a contact point with the substrate (Fig. 6c), usually form spherical shape to minimize the surface area. The orientation of the spherical nuclei does not contribute to the surface energy, therefore the non-wetting nuclei usually orient randomly [18]. For TiN, the amorphous phase forms a nearly uniform phase around the spherical nucleus surface, and the surface or interface energy of the film can be considered independent of the nuclei orientation. Therefore the nuclei are randomly oriented on the substrate.

These grains grow three dimensionally until they become large enough to come in contact with each other (Fig. 6d). Then the grains mainly grow along the direction normal to the substrate. Because the (200) plane in NaCl-structured TiN crystals is the plane of lowest surface energy [10], continuous films tend to change into (200) oriented films to minimize the surface energy. However, because it is often difficult for large grains to restructure in a short

period of time or at low temperature, the grains grow epitaxially along the direction normal to the substrate and form a columnar structure. Different crystal planes sometimes have different growth rates due to their different sticking probability of precursors. Under such conditions, competition occurs among the grains with different growth rates and only the grains with the highest growth-rate planes parallel to the substrate eventually survive. This phenomenon is also known as the “evolutionary selection rule” [19], which often appears in chemical vapor deposition (CVD). We therefore conclude that the preferred orientation evolves differently from thermodynamic predictions for d.c. sputtering, as shown in Figs. 4a and 6e.

For r.f. sputtering, however, after the grains become large enough to come in contact with each other, the films evolve into (200)-oriented films regardless of the N_2 partial pressure. That is, the (200) orientation is a necessary intermediate step even if (111)-oriented films appear later. Because of the stronger ion irradiation on film surfaces during r.f. sputtering compared with d.c. sputtering, this irradiation might cause the following three effects on the film, thus inducing a change in the thermodynamically favored (200) orientation.

1. Ion irradiation might increase the mobility of adatoms, thus promoting diffusion of atoms across grain boundaries and then anchor on the surface of (200)-oriented grains. This mechanism might be valid when the grain size is smaller than the diffusion length.
2. During initial contact or coalescence, ion irradiation might supply the energy for grains to restructure into thermodynamically stable structures, namely, (200)-oriented films.
3. Ion irradiation might damage the crystal structure of the grain surfaces and induce secondary nucleation. Contrary to the initial nucleation on the Si surface, the secondary nucleation on TiN presumably occurs in the wetting mode. The wetting nuclei have surface energy dependent on their orientation and thus the (200) orientation is preferred.

This irradiation effect only appears when the film is sufficiently thin (<20 nm, for instance), and it also tends to smoothen the film surface. Figures 4c (28 nm) and 6f indicate that films

deposited by using r.f. sputtering have (200) orientation with smooth surfaces. The increase in the substrate biasing voltage that caused the preferred orientation of TiN to change from (111) to (200) [12] implies that this ion irradiation effect can also be achieved by substrate biasing.

As the film thickness increases, the irradiation effect on the film structure weakens, and the kinetics dominates the film growth. The preferred orientation of the film will be developed by competitions among the grains. Because the effect of the N₂ partial pressure on the growth rate and on the preferred orientation was similar for both d.c. and r.f. sputtering (see Figs. 1 and 2), the relative growth rate of the (111) and (200) planes are probably affected by the N₂ partial pressure. Figures 6g and 6h indicate that the (111) and (200) orientations appear under low and high N₂ partial pressures, respectively.

V. CONCLUSIONS

The initial growth and texture formation mechanism of TiN films were investigated by using TEM and XRD. In the early stages of TiN deposition, randomly oriented nuclei were observed in a continuous TiN layer, which differs from the traditional island-growth of Volmer-Weber growth mode. After the nuclei grow and come in contact with each other to form a polycrystalline layer, the film exhibits various preferred orientations. When r.f. sputtering is used in the film deposition, the strong ion irradiation stimulates thin films to orient to a thermodynamically stable orientation. Whereas during d.c. sputtering, the grains grow epitaxially and form a columnar structure. The grains with the fastest growing plane parallel to the substrate dominate the other grains, causing the orientation of the film to assume the orientation of the fastest growing plane. According to this kinetic mechanism, TiN exhibits (111)-preferred orientation under relatively low N₂ partial pressure and (200)-preferred orientation under relatively high N₂ partial pressure. The (111) preferred orientation can also be obtained during early stages of deposition by selecting lower N₂ partial

pressures and d.c. sputtering that result in reduced ion irradiation.

Acknowledgements

This work was supported by the “Research for the Future” Program of the Japan Society for the Promotion of Science (JSPS-RFTF 96P00402). We thank Profs. Y. Yamaguchi, Y. Shimogaki, Y. Ikuhara, and T. Okubo for helpful discussions and comments. We also thank Mr. Y. Ogawa for instruction of the TEM operation.

References

- [1] S.P. Murarka, R.J. Gutmann, A.E. Kaloyeros and W.A. Lanford, *Thin Solid Films* 236 (1993) 257.
- [2] M. Kageyama, K. Hashimoto, and H. Onoda, 26th IEEE/IRPS Conference Proceeding, 1991, p. 97.
- [3] S. Vaidya and A.K. Sinha, *Thin Solid films* 75, 253 (1981).
- [4] M. Tsukada and S. Ohfuji, *J. Vac. Sci. Technol. B* 11, 326 (1983).
- [5] H. Onoda, M. Kageyama, and K. Hashimoto, *J. Appl. Phys.* 77, 885 (1995).
- [6] H. Onoda, M. Kageyama, and K. Hashimoto, *J. Appl. Phys.* 32, 4479 (1993).
- [7] D.P. Tracy, D.B. Knorr, and K.P. Rodbell, *J. Appl. Phys.* 76, 2671(1994).
- [8] D.B. Knorr, S.M. Merchant, and M.A. Biberger, *J. Vac. Sci. Technol. B* 16(5), 2734 (1998).
- [9] U.C. Oh and Jung Ho Je, *J. Appl. Phys.* 74(3), 1692(1993).
- [10] J. Pelleg, L.Z. Zevin, and S. Lungo, *Thin Solid Films* 197, 117(1991).
- [11] J.H. Je, D.Y. Noh, H.K. Kim, K.S. Liang, *J. Mater. Res.*, vol. 12, 9(1997).
- [12] P. Patsalas, C. Charitidis, S. Logothetidis, *Surf. Coat. Technol.* 125 (2000) 335.
- [13] H. H. Yang, J. H. Je, K. B. Lee, *J. Mater. Sci. Lett.* 14(1995) 1635-1637.
- [14] Li-Jian Meng, M.P. dos Santos, *Surf. and Coat. Tech.* 90(1997)64-70.

- [15] Rh.Roquiny, G.Mathot, G.Terwagne, F.Bodart, P.van den Brande, Nucl. Ins. Methods in Phys. Res. B 161-163 (2000) 600-604.
- [16] Shiqin Xiao, Cristian P. Lungu, Osamu Takai, Thin Solid Films 334(1998) 173-177.
- [17] I. Petrov, A. M. Myers, J. E. Greene, and J. Abelson, J. Vac. Sci. Technol. A 12, 2846 (1994).
- [18] H. Shirakawa, H. Komiyama, J. Nanoparticle Research 1 (1999) 17.
- [19] A. van der Drift, Philips Res. Repts 22, 267-288, 1967.

Figure Captions

Table 1: Deposition conditions for TiN growth

Table 2: Effect of film thickness on orientation of films deposited under conditions shown in Table 1.

Fig. 1 Effect of N_2 partial pressure on TiN deposition rate.

Fig. 2 Effect of N_2 partial pressure on the texture of films deposited by using (a) d.c. and (b) r.f. sputtering.

Fig. 3 TEM micrographs of TiN films deposited by using d.c. sputtering for 10 s, (a) is the cross-sectional image, (b) is the pane-view image, and (c) is an amplified nuclei with amorphous phase around it.

Fig. 4 XTEM micrographs of TiN films deposited by using d.c. sputtering for (a) 30 s, (b) 120 s, and (c) is deposited by using r.f. sputtering for 180 s.

Fig. 5 Effect of film thickness on preferred orientation of films deposited by using (a) d.c. and (b) r.f. sputtering.

Fig. 6 Schematic of TiN film growth. Initially, continuous amorphous layer deposition is supposed to occur, followed by the nucleation with random orientation in it (a). The cases of wetting (b) and non-wetting (c) nuclei are also shown in comparison. As the grains grow larger, they contact with each other to form the randomly oriented continuous microcrystalline layer (d) and then the preferred orientation evolves dependently on the deposition conditions (e, f). Finally the film comes to have columnar structures with some preferred orientations depending on the N_2 partial pressure (g, h).

TABLE 1

TABLE I. Deposition conditions of the samples used for investigation of TiN growth.

	Condition I	Condition II
Power (W)	dc 69	rf 100
Total pressure (Pa)	0.9	0.9
N ₂ partial pressure (Pa)	0.047	0.015
Deposition rate (nm/s)	0.19	0.26

TABLE 2

TABLE II. Changes of the orientation with film thickness under the deposition conditions in Table I.

Film thickness	dc (Condition I)	rf (Condition II)
~ 3 nm	Random	Random
~ 20 nm	111	200
Thick film (>50 nm)	111 (50 nm)	111 (110 nm)

Fig. 1

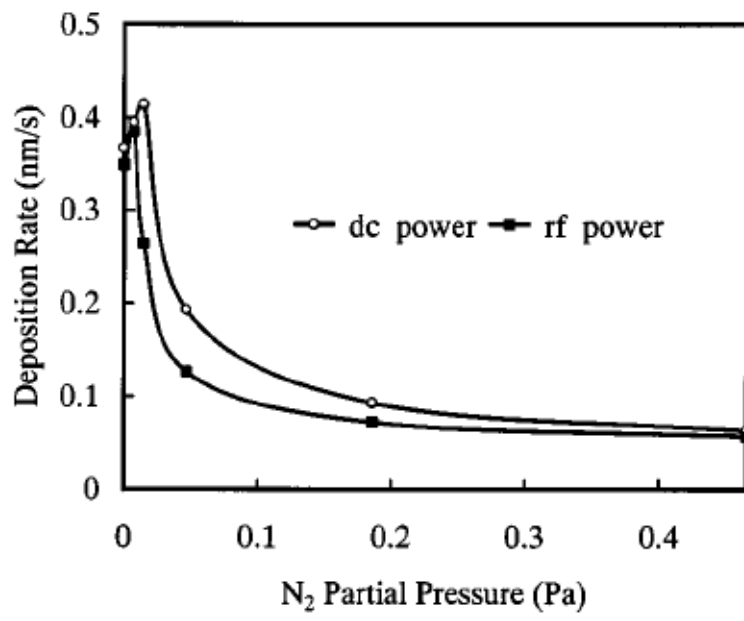


Fig. 2

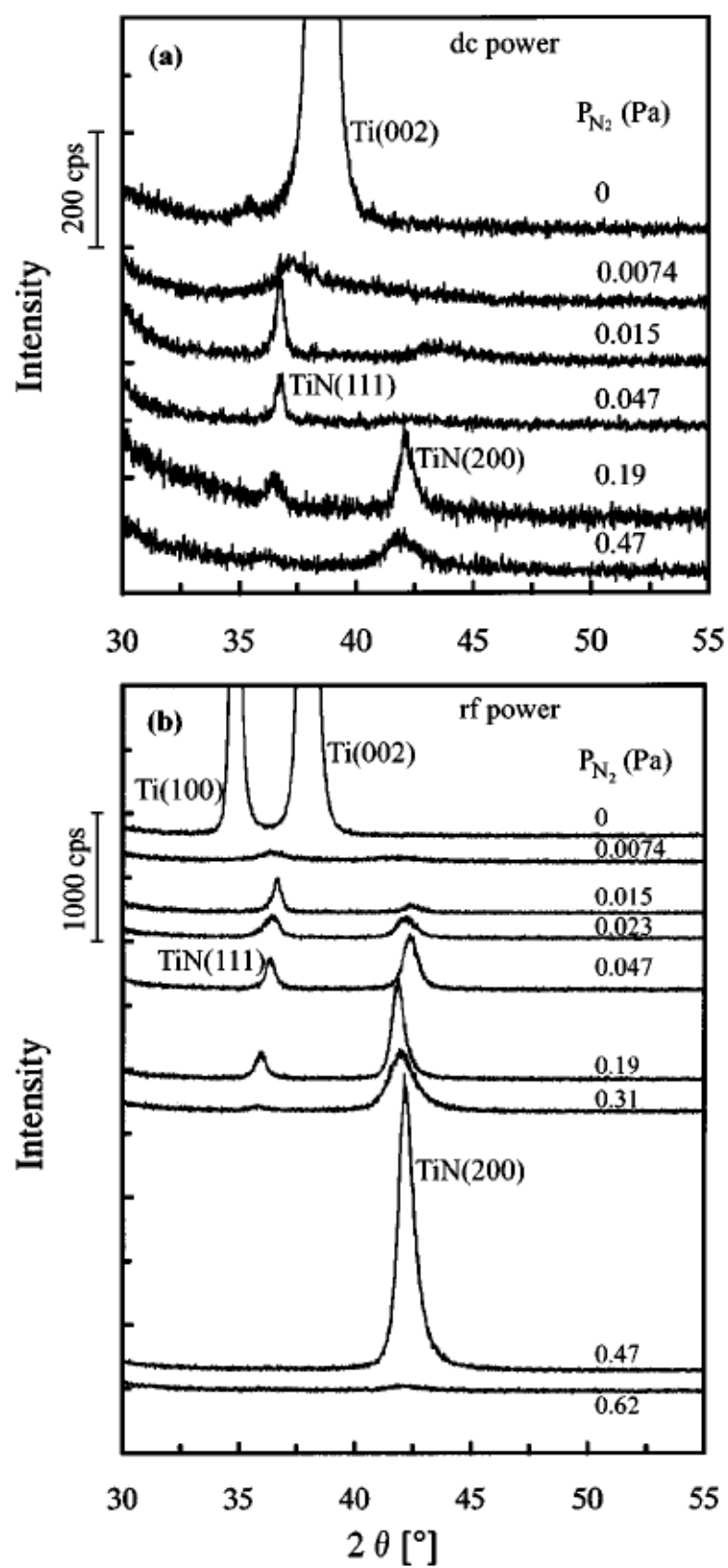


Fig. 3

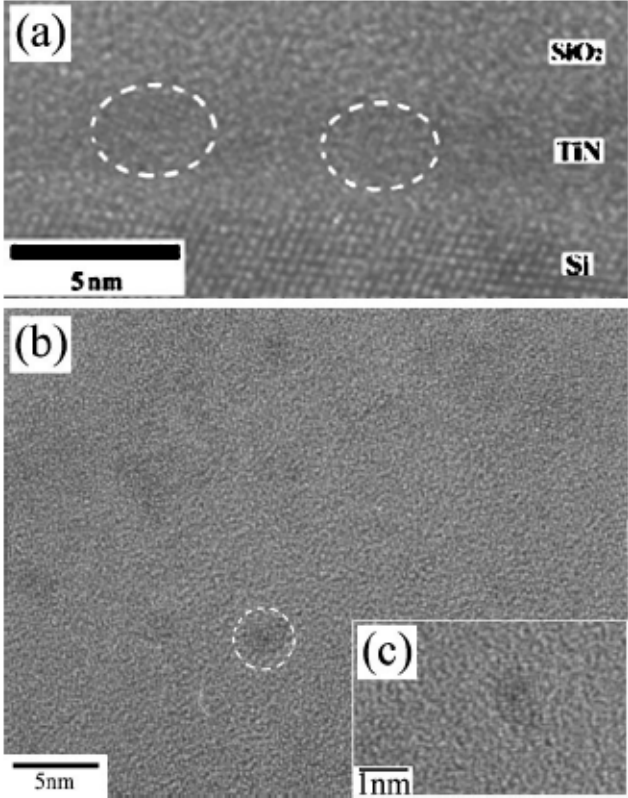


Fig. 4

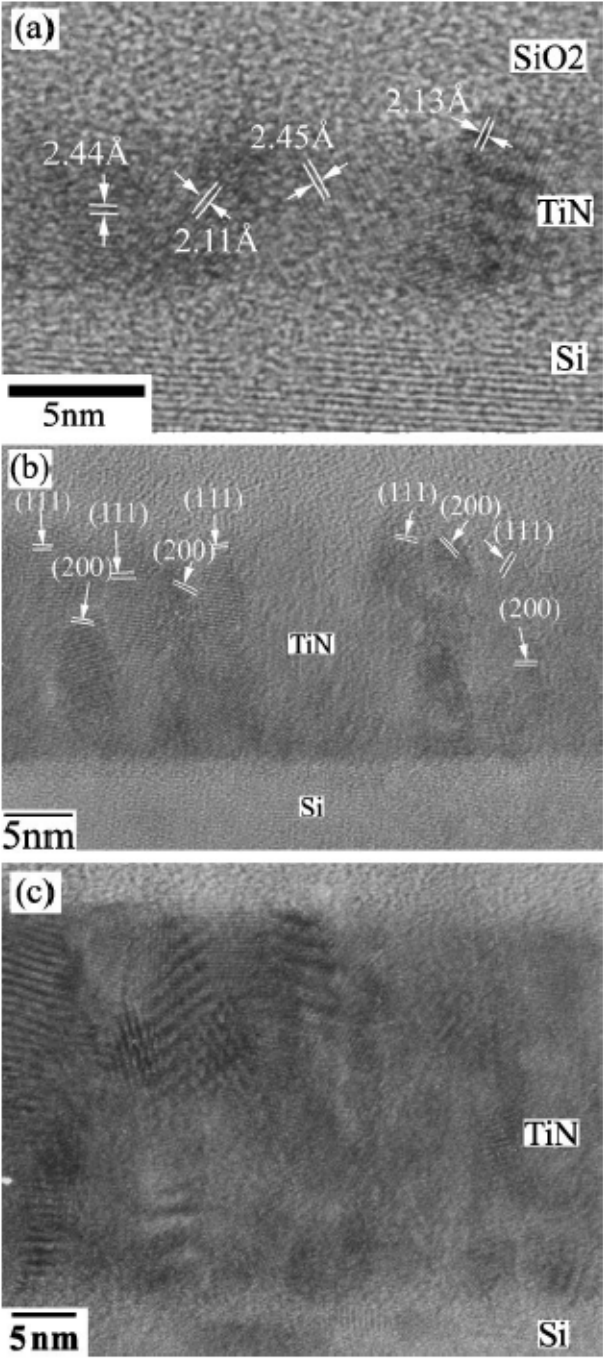


Fig. 5

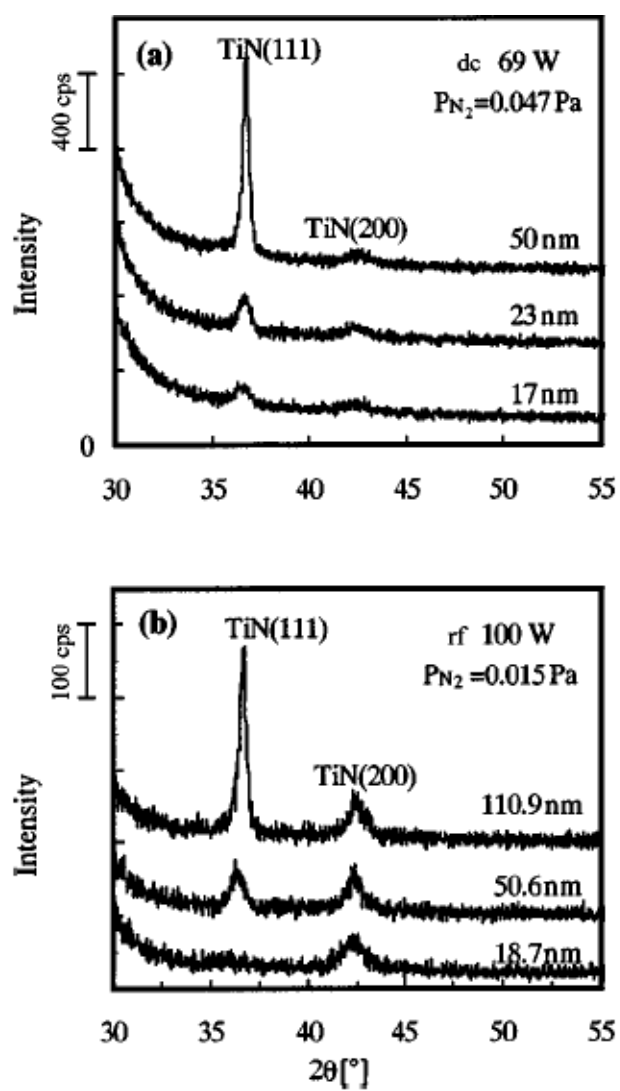


Fig. 6

